Journal of Surgical Research **89,** 43–52 (2000)
doi:10.1006/jsre.1999.5799, available online at http://www.idealibrary.com on IDEAL®

Use of Mathematical Model to Predict Hemodynamics in Cavopulmonary Anastomosis with Persistent Forward Flow[1]

Giancarlo Pennati, Ph.D.,* Francesco Migliavacca, Ph.D.,† Gabriele Dubini, Ph.D.,‡
Riccardo Pietrabissa, Ph.D.,* Roberto Fumero, M.Sc.,* and Marc R. de Leval, M.D., FRCS†

**Dipartimento di Bioingegneria, and ‡Dipartimento di Energetica, Politecnico di Milano, 20133 Milan, Italy; and †Cardiothoracic Unit, Great Ormond Street Hospital for Children NHS Trust, London, United Kingdom*

Submitted for publication September 20, 1999

Background. **The bidirectional cavopulmonary anastomosis with additional pulmonary blood flow is used as a staged procedure or a definitive palliation of univentricular hearts. In this paper the flow competition occurring between the caval and the pulmonary flows is investigated. The hemodynamics in the superior vena cava and the blood flow distribution into the lungs, as well as the systemic arterial oxygen availability, are correlated with the severity of the right ventricle outflow tract obstruction and the pulmonary arteriolar resistance.**

Materials and methods. **Computer models of the pre- and postoperative hemodynamics of univentricular hearts were developed. The effects of increasing severity of the right ventricle outflow tract obstruction, with a pulmonary arteriolar resistance ranging from 0.8 to 7.9 nonindexed Woods units, were simulated.**

Results. **The study indicates that the presence of an additional pulmonary blood flow from the native pulmonary artery may be beneficial. Since an excessive additional blood flow may cause central venous hypertension, its optimal value should be chosen according to the value of pulmonary arteriolar resistance. The model was utilized to simulate four clinical cases.**

Conclusions. **The simulations show that the model can predict the postoperative hemodynamics and could therefore be usefully applied to predict quantitatively the effect of the native pulmonary blood flow following bidirectional cavopulmonary anastomosis.**

Key Words: **congenital heart diseases; bidirectional cavopulmonary anastomosis; hemodynamics; computer model.**

[1] This work was supported in part by the British Heart Foundation and in part by the Italian 'Ministero dell'Università e della Ricerca Scientifica e Tecnologica' (MURST).

INTRODUCTION

Surgical repairs of complex heart defects may involve major reconstructive procedures, creating new cardiovascular anatomy and hemodynamics. Right heart by-pass operations for hearts that have in common the presence of a single usable ventricular chamber are one of many examples.

Typically these repairs consist of a partial (bidirectional cavopulmonary anastomosis, BCPA) or total (total cavopulmonary connection) derivation of the systemic venous return to the pulmonary arteries [1, 2]. The BCPA [3] is frequently utilized in the staged surgical management of univentricular hearts. Whereas some surgeons insist on closing any other source of pulmonary blood flow while performing a BCPA, others maintain patency of either a stenosed native pulmonary outflow or of a systemic to pulmonary arterial shunt. Whether an additional source of pulmonary blood flow (ABF) can safely and usefully be left at the time of the BCPA to increase systemic saturation or must be eliminated to reduce the volume load on the ventricle remains controversial [4].

The theoretical advantages of providing ABF are twofold: a better systemic arterial saturation and a large period of palliation. The drawbacks are threefold: the risk of systemic venous hypertension in the upper body, side effects of competitive flow between superior vena cava, and forward flow and the chronic volume overload on the ventricular chamber.

We have developed a policy of maintaining ABF while performing a BCPA. A retrospective study of 107

0022-4804/00 $35.00

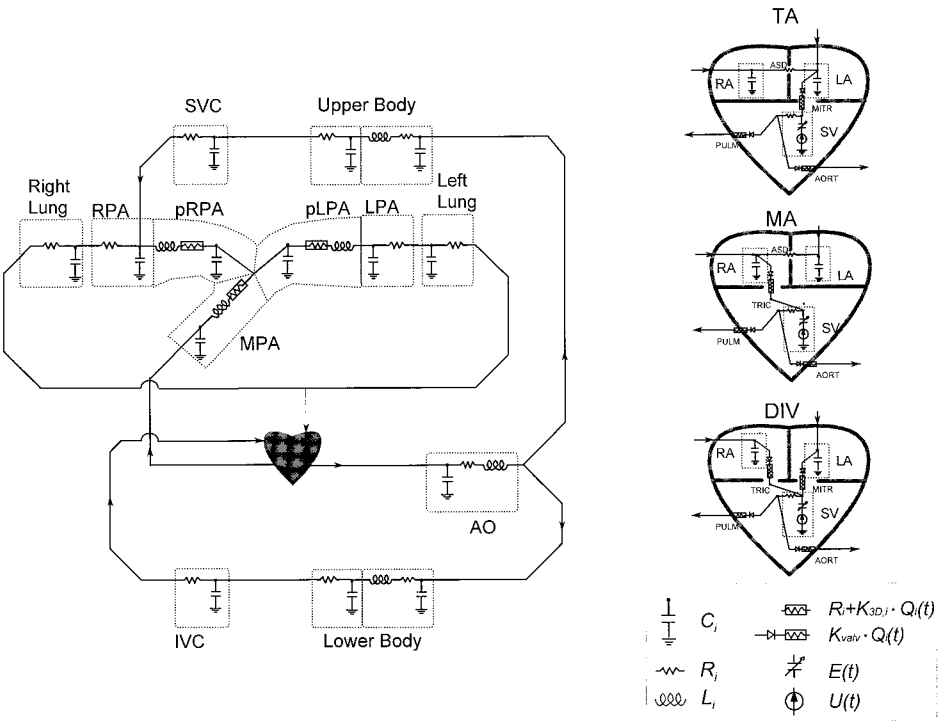

FIG. 1. (Left) Hydraulic network of the postoperative model with the bidirectional cavopulmonary anastomosis. Arrows indicate the normal direction of flow. The values of the pulmonary parameters in the shaded area are evaluated from three-dimensional mathematical models of the connection (see text). (Right) Models of the tricuspid atresia (TA) (top), mitral atresia (MA) (middle), and double inlet ventricle (DIV) (bottom). AO, ascending aorta; AORT, aortic valve; ASD, atrial septal defect; IVC, inferior vena cava; LA, left atrium; LPA, left pulmonary artery; MITR, mitral valve; MPA, main pulmonary artery; pLPA and pRPA, proximal left and right pulmonary artery; PULM, pulmonary valve; RA, right atrium; RPA, right pulmonary artery; SV, single ventricle; SVC, superior vena cava; TRIC, tricuspid valve.

patients showed that approximately 20% had too high venous pressure and excessive forward flow [4].

Although animal and *in vitro* experimentations have been carried out, computational fluid dynamics (CFD) modeling was used in the present study to predict postoperative hemodynamics from preoperative clinical data [5].

To study the reciprocal effects of the local fluid dynamics and the rest of the circulation, a three-dimensional model of BCPA plus forward flow [4, 6, 7] was incorporated in a lumped parameter model representing the overall circulation.

METHODS

Lumped parameter models of absent atrioventricular connection (tricuspid atresia (TA) or mitral atresia (MA)) and double inlet ventricle (DIV), before and after BCPA were constructed on the basis of previous computational work [8]. The models were divided into three regions: the heart, the systemic, and the pulmonary circulation. The whole hydraulic network of the BCPA (postoperative) model is illustrated in Fig. 1.

Each circulatory region was divided into several compliant districts: five for the systemic circulation and seven for the pulmonary circulation. The hydraulic behavior of each district was mathematically modeled on the basis of mass and momentum conservation laws, which lead to two differential equations where the dependent variables are the volume flow rate $Q(t)$ and pressure $P(t)$, both functions of time (for details, see Appendix 1).

The following general assumptions were made: (i) the vascular districts have a constant compliance; (ii) the blood is an incompressible (density $\rho = 1.06$ g/cm^3), viscous, and Newtonian fluid (viscosity $\mu = 0.03$ g/(cm · s)); and (iii) the flow in the vessels is laminar.

The heart. The ventricle was represented (Appendix 1) according to Avanzolini *et al.* [9] as an isovolumic time-varying pressure generator $U(t)$ (contractility) coupled with a constant viscous term R_v (related to the dissipative properties of the myocardium) and a time-varying, elastic term $E(V,t)$ (related to the nonlinear tension–length curve of the activated fiber and the geometry of the ventricle). The atria were modeled with a constant compliance disregarding their contractility. A nonrestrictive atrial septal defect (ASD) was built in the TA and MA models. Flows through the atrioventricular and arterial valves were described by a nonlinear relationship between the pressure drop and the volume flow rate across them (Appendix 1).

Values for heart parameters used for the calculations were extrapolated from data available in the literature [9–11].

The systemic circulation. The systemic circulation was divided into five districts (Fig. 1): the ascending aorta (AO), the upper and lower part of the body (upper body and lower body) in parallel, each containing an arterial and a venous sector, and the caval veins (SVC and IVC, respectively). Resistance R, compliance C, and inertance L (RCL block) were entered in the arterial model, whereas resistance and compliance only were entered in the venous system, assuming negligible flow inertia. After the BCPA, the SVC is connected to the

TABLE 1

Preoperative Data from 10 Patients with Univentricular Heart

	Mean ± SD	Range
Age (years)	3.7 ± 3.0	0.6–9.0
BSA (m^2)	0.6 ± 0.2	0.3–0.8
SVR (Woods unit)[a]	21.7 ± 15.6	12.7–48.6
PAR (Woods unit)	2.2 ± 2.0	0.9–5.3
HR (bpm)	100 ± 20	83–130

Note. 1 Woods unit = 1 mm Hg/(L/min) = 8 Pa/(cm^3/s).

right pulmonary artery (RPA), whereas the IVC remains connected to a compliant chamber made of the RA.

The pulmonary circulation. The pulmonary arterial circulation was divided into seven districts (MPA, pLPA, pRPA, LPA, and RPA districts, and left and right lungs, Fig. 1), with one RCL block for the central pulmonary arteries and RC block for the peripheral pulmonary artery and another block for the lungs and pulmonary veins. The pressure drop across each of the proximal pulmonary arterial districts (MPA, pRPA, and pLPA) takes into account the complex local hemodynamics (Appendix 1). Values for the included inertance (L_i) and resistance (R_i and $K_{3D,i}$) coefficients were derived from our previous three-dimensional CFD simulations [4, 6–8].

Numerical simulations. Preoperative cardiac catheterization data of 10 children with univentricular hearts were used to construct the model and included: the body surface area (BSA), the systemic vascular resistance (SVR), the pulmonary arteriolar resistance (PAR), and the heart rate (HR). The data expressed as means ± SD are summarized in Table 1.

Systemic and pulmonary vascular parameters within each various district were obtained from previously published models [8, 12–15]. These data were then incorporated in the preoperative computational model.

Simulations were carried out on the BCPA model to evaluate the role of the pulmonary arteriolar resistance (ranging from 0.8 to 7.9 Woods units) and the severity of the degree of right ventricle outflow tract obstruction (RVOTO). Postoperative models with 50, 60, 75, and 100% RVOTO were investigated. A 100% RVOTO corresponds to pulmonary atresia, whereas the 50, 60, and 75% represent various degrees of discrete pulmonary stenoses comparable to a pulmonary arterial banding, leading to different pressure drops ($\Delta P_{syst} \leq 40$ mm Hg, $\Delta P_{syst} = 40 \div 60$ mm Hg, and $\Delta P_{syst} \geq 60$ mm Hg, respectively, where ΔP_{syst} is the systolic pressure drop between the single ventricle and the pulmonary arteries).

The prediction of hemodynamics uses, as input for the model, the following preoperative data: BSA, HR, PAR, SVR, and RVOTO. The BCPA with pulmonary ABF is then simulated, from which the following data were derived: the pressure in the superior vena cava (P_{SVC}) and in the pulmonary arteries (P_{LPA} and P_{RPA}), the pulmonary-to-systemic flow ratio (Q_p/Q_s), the volume flow rate in the SVC (Q_{SVC}) and in the pulmonary arteries (Q_{RPA} and Q_{LPA}), the right-to-left lung flow ratio (Q_r/Q_l), the SVC-to-pulmonary flow ratio (Q_{SVC}/Q_p), and the cardiac output (CO). The cardiac output was calculated as the sum of the aortic (Q_s) and the pulmonary cardiac outflows (Q_{MPA}).

From the above postoperative hemodynamic data, in particular Q_s and Q_p/Q_s, the systemic arterial oxygen availability (SAOA) and the percentage of systemic arterial oxygen saturation (Sat_{art}) can be calculated (see Appendix 2):

$$SAOA = Q_s \cdot \frac{Sat_{PV}}{100} \cdot OxCap - \frac{(\alpha_{LB} \cdot C\dot{V}O_2)}{(Q_p/Q_s)}, \quad (1)$$

$$Sat_{art} = \frac{SAOA}{Q_s \cdot OxCap} \cdot 100. \quad (2)$$

These calculations only require the knowledge of the percentage of pulmonary venous oxygen saturation (Sat_{PV}), the fraction (α_{LB}) of the systemic oxygen consumption ($C\dot{V}O_2$) due to lower body, and the maximal oxygen capacity (OxCap).

The algebraic–differential system of equations of the model was treated with an interactive program for simulating dynamical systems (SIMNON, SSPA System, Lund, Sweden). Computations were carried out on a Pentium II PC with 32 Mb RAM. Time computation for a typical simulation took less than 15 s.

RESULTS

Results from simulations of pre- and postoperative DIV circulation with a 50% RVOTO are shown in Figs. 2 and 3. Preoperative input and output data are summarized in Table 2. Figure 2 displays the pressure and flow tracings in the SVC. Following the BCPA, the SVC pressure rises and shows a higher pulsatility than in the preoperative model. There is retrograde postoperative flow in the SVC in systole for RVOTO of 50%. Postoperative SVC pulsatility is clearly transmitted by the pulsatile flow in the pulmonary arteries. Figure 3 illustrates the pre- and postoperative instantaneous pressure in the RPA and LPA. Differences in pressure patterns within the pulmonary arteries were noted: the RPA pressure is damped compared to the LPA.

Figures 2 and 3 also show the effects of increasing RVOTO (50, 75, and 100%) on the postoperative hemodynamics, for PAR of 2.2 Woods units. The effects of increasing pulmonary arteriolar resistance (0.8, 2.2, 4.9, and 7.9 Woods units) in the presence of various

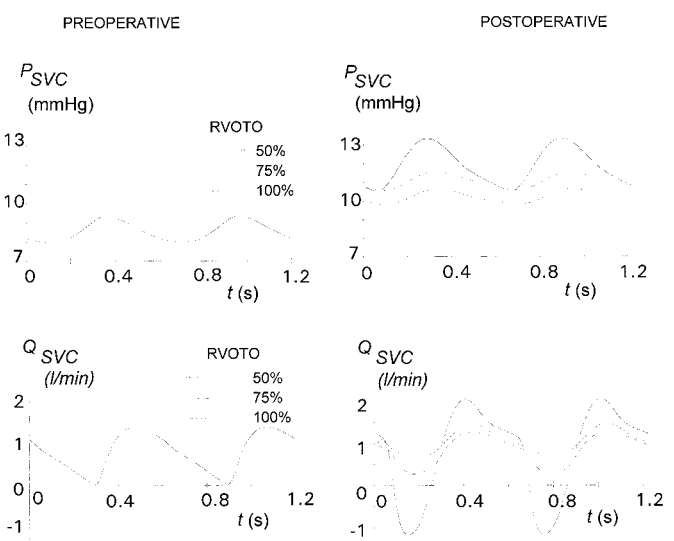

FIG. 2. Pressure and flow tracings in the superior vena cava (SVC) for the preoperative (left) and postoperative (right) situations. BSA equal to 0.6 m^2, PAR equal to 2.2 Woods units, SVR equal to 21.7 Woods units, and HR = 100 bpm.

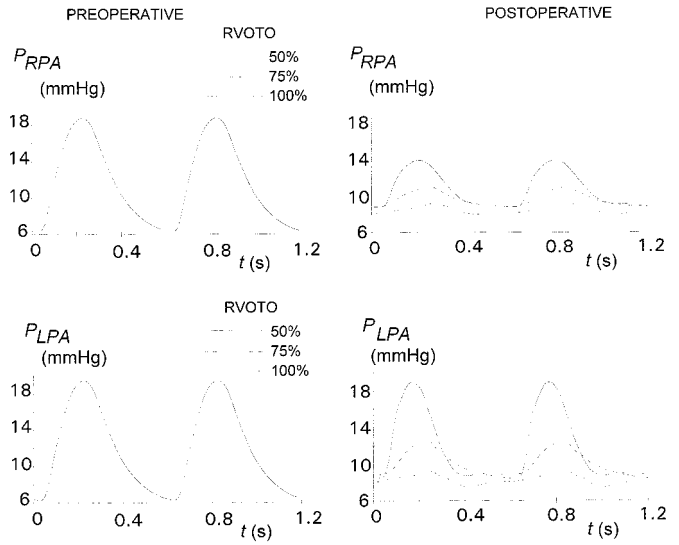

FIG. 3. Pressure tracings in the left (LPA) and right (RPA) pulmonary arteries for the preoperative (left) and postoperative (right) situations. BSA equal to 0.6 m^2, PAR equal to 2.2 Woods units, SVR equal to 21.7 Woods units, and HR = 100 bpm.

degrees of RVOTO are shown in Table 3. SAOA and Sat_{art}, calculated using Sat_{PV} = 98%, OxCap = 20 ml oxygen/100 ml, and $\alpha_{LB} \cdot CVO_2$ = 62.5 ml oxygen/min, are reported in the same table. As PAR increases, CO, Q_p/Q_s ratio, Q_{SVC}/Q_p ratio, SAOA, and Sat_{art} decrease, whereas the mean SVC pressure monotonically increases. With regard to increasing degrees of RVOTO, SAOA and Sat_{art} exhibit an opposite trend. The ratio between the mean flow to the right lung and that to the left one was calculated separately during diastole (Q_r/

TABLE 2

Data for the Typical Preoperative Situation

Input data	
BSA (m^2)	0.6
HR (bpm)	100
PAR (Woods unit)	2.2
SVR (Woods unit)	21.7
RVOTO (%)	50
Output data	
ΔP_{syst} (mm Hg)	35
Q_p (L/min)	2.07
Q_s (L/min)	1.67
CO (L/min)	3.74
Q_p/Q_s	1.24
Q_r/Q_l	0.92
P_{SVC} (mm Hg)	8.6

Note. BSA, body surface area; HR, heart rate; PAR, pulmonary arteriolar resistance; SVR, systemic vascular resistance; RVOTO, right ventricle outflow tract obstruction; P_{SVC}, mean superior vena cava pressure; Q_p and Q_s, mean pulmonary and systemic blood flow rate; Q_r and Q_l, mean right and left pulmonary blood flow rate; ΔP_{syst}, systolic pressure gradient across the pulmonary outflow obstruction.

TABLE 3

Hemodynamic Results in Postoperative Models as Functions of PAR and Severity of the Right Ventricle Outflow Obstruction (RVOTO)

	RVOTO (%)	PAR (Woods unit) 0.8	2.2	4.9	7.9
P_{SVC} (mm Hg)	50	9.6	12.0	16.0	19.2
	60	9.3	11.5	15.1	18.2
	75	8.9	10.9	14.2	17.1
	100	8.2	9.2	11.1	12.9
CO (L/min)	50	3.44	3.24	2.89	2.60
	60	3.17	2.99	2.71	2.46
	75	2.89	2.74	2.51	2.31
	100	2.03	1.97	1.88	1.80
Q_p (L/min)	50	2.65	2.45	2.11	1.84
	60	2.34	2.17	1.90	1.67
	75	2.03	1.89	1.68	1.49
	100	1.01	0.97	0.88	0.83
Q_s (L/min)	50	1.53	1.45	1.33	1.22
	60	1.60	1.52	1.40	1.29
	75	1.67	1.59	1.47	1.36
	100	2.03	1.97	1.88	1.80
Q_p/Q_s	50	1.73	1.69	1.59	1.50
	60	1.46	1.43	1.36	1.29
	75	1.21	1.19	1.15	1.10
	100	0.50	0.49	0.47	0.46
Q_r/Q_l	50	0.87	0.85	0.89	0.91
	60	0.92	0.90	0.92	0.94
	75	1.00	0.98	0.97	0.97
	100	1.33	1.13	1.06	1.03
Q_{SVC}/Q_p	50	0.28	0.27	0.26	0.25
	60	0.33	0.32	0.31	0.30
	75	0.40	0.39	0.38	0.36
	100	1.00	1.00	1.00	1.00
Q_r/Q_{l-dias}	50	1.62	1.23	1.12	1.08
	60	1.30	1.23	1.11	1.08
	75	1.18	1.08	1.03	1.01
	100	1.38	1.12	1.08	1.01
Q_r/Q_{l-syst}	50	0.72	0.73	0.79	0.84
	60	0.87	0.77	0.84	0.87
	75	0.89	0.91	0.93	0.93
	100	1.27	1.08	1.01	1.00
SAOA (ml oxygen/min)	50	263	246	220	197
	60	270	252	227	204
	75	275	257	231	208
	100	271	257	234	215
Sat_{art} (%)	50	86	85	83	81
	60	85	84	81	79
	75	82	81	79	77
	100	67	65	62	60

Note. CO, total ventricular outflow; PAR, pulmonary arteriolar resistance; P_{SVC}, mean superior vena cava pressure; Q_p and Q_s, mean pulmonary and systemic blood flow rate; Q_r and Q_l, mean right and left pulmonary blood flow rate; Q_{SVC}, mean superior vena cava blood flow rate; SAOA, systemic arterial oxygen availability; Sat_{art}, percentage of arterial blood saturation; dias, diastolic; syst, systolic.

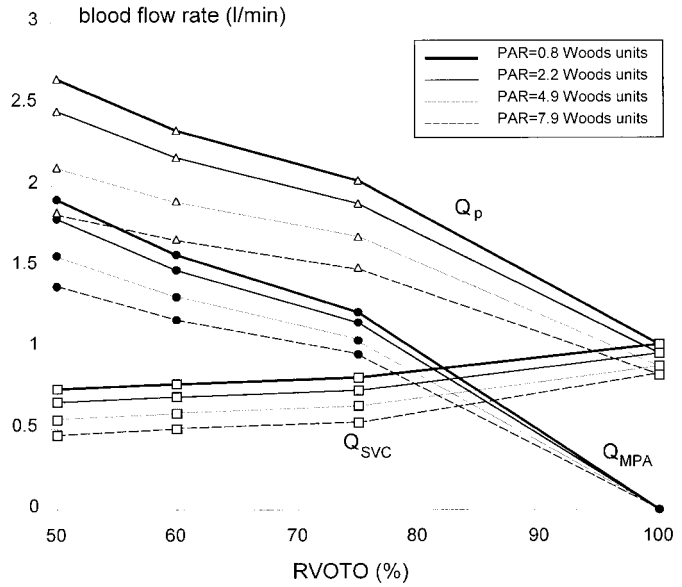

FIG. 4. Combined effects of changes in the right ventricular outflow tract obstruction (RVOTO) and pulmonary arteriolar resistance (PAR) upon the pulmonary flow (Q_p), the superior vena caval flow (Q_{SVC}), and the main pulmonary artery flow (Q_{MPA}).

Q_{l-dias}) and systole (Q_r/Q_{l-syst}) and they are reported in Table 3, as well. During diastole the flow toward the right lung is prevalent and decreases with increasing values of the PAR and the severity of the pulmonary outflow obstruction. During systole an opposite trend occurs, except for the simulation with the absence of the pulmonary ABF (100% RVOTO).

The combined effects of changes of RVOTO and PAR on the two sources of pulmonary flow, namely Q_{SVC} and Q_{MPA}, are depicted in Fig. 4, while those on the predicted postoperative P_{SVC}, Q_s, and Q_p/Q_s (Table 3) are depicted in a diagrammatic format in Fig. 5. The latter diagram was constructed for BSA of 0.6 m^2, HR of 100 bpm, and SVR of 21.7 Woods units. The white areas represent the regions where Q_p/Q_s ranges between 0.75 and 1.25, Q_s between 1.5 and 2.0 L/min, and the mean P_{SVC} is lower than 15 mm Hg. If, for example, the value of PAR is less than 4 Woods units, a tighter band will be required to optimize surgical outcome.

Clinical Validation

The model was tested on four clinical cases summarized in Table 4. Validation of computational modeling was made on the pre- and postoperative hemodynamic measurements and this is represented in Table 5. It shows a fairly good correlation for all the four cases both pre- and postoperatively.

Patient 1 is a particularly good example of a child with DIV and banded MPA who had an elevated PAR (14.9 Woods units) and PA pressure. The SVC pressure was 25 mm Hg at the completion of the BCPA and the proximal RPA was then occluded so as to divert the SVC flow to the right lung and the forward flow from the native pulmonary outflow tract to the left lung.

DISCUSSION

The aim of the study was to predict the postoperative hemodynamics of a BCPA in the presence of a forward flow from the native pulmonary artery with particular attention to the SVC pressure. A mathematical model of the whole circulation system as a closed loop, composed of lumped resistance, compliance, and inertance elements, was developed. Nonlinear elements describing the local hemodynamics at the pulmonary bifurcation and the caval anastomosis were derived from previous studies, based on the use of the finite element method [4, 6, 7]. In other words, details on the local flow field at the anastomosis were computed by means of the three-dimensional model and then "condensed" into a group of nonlinear parameters in the closed loop [8]. The closed loop allowed to evaluate the mutual interactions between several hemodynamics variables. Adoption of such a model is crucial as it gives a full picture of the hemodynamics responses to changes in a single circulatory parameter. This is well illustrated in Fig. 4, which shows that an increasing RVOTO causes a reduction in the flow through the main pulmonary artery (Q_{MPA}), but also an increase of the systemic flow, hence of that from SVC (Q_{SVC}). To some extent, the latter compensates for the former.

This kind of information cannot be given by a standalone three-dimensional model of the anastomosis (based on the use of the finite element method), which requires to prescribe Q_{SVC} and Q_{MPA} flows as known quantities [4, 6, 7]. Our study suggests that a proper regulation of the RVOTO could optimize the hemodynamics at each value of pulmonary resistance.

Agreement between our simulation and the four clinical cases is fairly good. Our model is able to predict the changes occurring in the hemodynamics after BCPA. In the first three patients the agreement between the measured and the predicted postoperative SVC pressure is satisfactory. Q_p/Q_s and Q_s, respectively, close to unity and above 1.3 L/min, agree with the satisfactory outcome reported after surgery. Patient 4 simulation showed that the model evaluated Q_p/Q_s and Q_s trends correctly, in addition to that of the SVC pressure.

This model also allows a straightforward estimation of oxygen transport on the basis of blood flow calculations. For instance, the model indicates that at constant PAR, slightly higher SAOA can be achieved with a degree of RVOTO passing from 50 to 75%, although Sat_{art} decreases, and provided that the MPA is not ligated (Table 3). This could appear rather peculiar, but it can be explained considering that increasing severity of the RVOTO causes Q_s (and hence SAOA) to

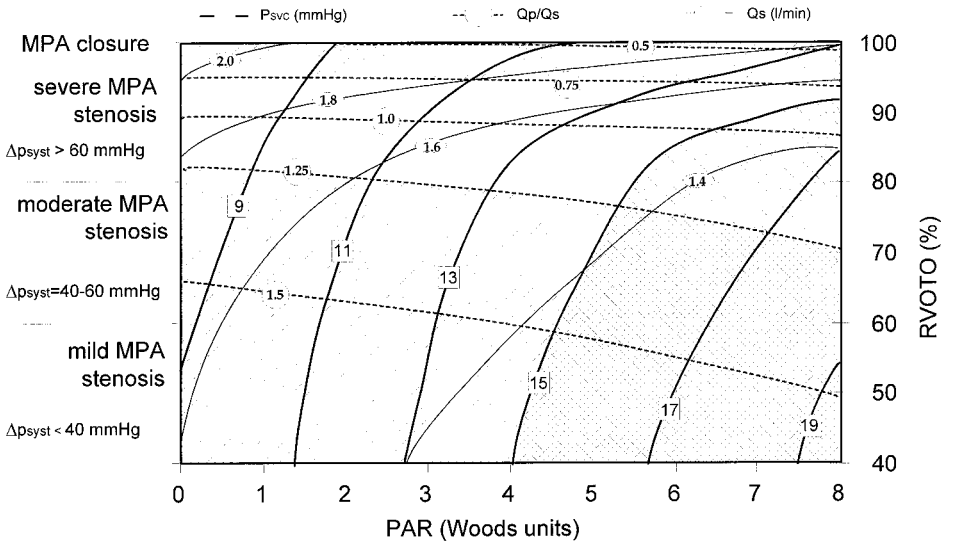

FIG. 5. Map with areas corresponding to different possible surgical outcomes after the BCPA as functions of the pulmonary arteriolar resistance (PAR) and the preoperative systolic pressure gradient across the pulmonary outflow obstruction (ΔP_{syst}). The latter is discretized into three intervals, roughly corresponding to a mild stenosis ($\Delta P_{syst} \leq 20 \div 40$ mm Hg), a moderate stenosis ($\Delta P_{syst} = 40 \div 60$ mm Hg), and a severe stenosis ($\Delta P_{syst} \geq 60$ mm Hg). See text for explanation. The white area indicates the optimal surgical outcome, with a postoperative Q_p/Q_s in a range between 0.75 and 1.25 and a postoperative P_{SVC} lower than 15 mm Hg. The darkest shaded area represents the postoperative conditions with P_{SVC} greater than 15 mm Hg and a Q_p/Q_s ratio outside the above range, simultaneously.

increase. Furthermore, one should note that prediction based only on the postoperative Sat_{art} is inadequate, as the quantity of oxygen delivered to the body also depends on the mean systemic flow rate Q_s. This was the main reason for SAOA to be introduced. A similar approach has already been applied by Santamore and colleagues [16], but their model does not describe how the values for Q_p/Q_s and CO can be achieved.

Model simulations also indicate that closure of ABF is not beneficial to the arterial saturation, although useful to reduce the pressure in the SVC. Indeed, calculated arterial saturation reaches values which appear very low (60–67%). In our view, this depends on the assumption on the oxygen consumption (Eqs. (1) and (2)).

The clinical applicability of our modeling is also supported by clinical observations previously published [17–19].

TABLE 4

Data from Four Clinical Cases Used for the Validation of the Computational Model

						Preoperative data		
Patient	BSA (m^2)	Age	Weight (kg)	Diagnosis	Previous operations	PAR (Woods)	SVR (Woods)	ΔP_{sys} (mm Hg)
1	0.5		13.1	DIV, TGA, ASD, subaortic stenosis, right AV valve regurgitation, small left AV valve	PA banding	14.9	23.5	30
2	0.8		18.8	DIV, TGA	PA banding	0.85	21.4	66
3	0.5	4 years	14.5	HRV, unbalanced AVSD	Straddling right sided AV valve	3.5	22.4	80
4	0.39	10 months	7.6	DORV with MA, HLV	Atrial septectomy, PA banding	12	57	60

Note. DIV, double inlet ventricle; DORV, double outlet right ventricle; PA, pulmonary artery; TGA, transposition of great arteries; ASD, atrial septal defect; AVSD, atrioventricular septal defect; AV, atrioventricular; HRV, hypoplastic right ventricle; HLV, hypoplastic left ventricle; MA, mitral atresia; PAR, pulmonary arteriolar resistances; SVR, systemic vascular resistances; ΔP_{sys}, pulmonary gradient. 1 Woods unit = 1 mm Hg/L/min.

TABLE 5

Clinical and Predicted Data for the Four Clinical Cases Tested

	Clinical data						Predicted simulated data					
	Preoperative			Postoperative			Preoperative			Postoperative		
Patient	Q_s (L/min)	Q_p/Q_s	Pressure (mm Hg)	Q_s (L/min)	Q_p/Q_s	Pressure (mm Hg)	Q_s (L/min)	Q_p/Q_s	Pressure (mm Hg)	Q_s (L/min)	Q_p/Q_s	Pressure (mm Hg)
1	2.2	1	SV = 51/9 MPA = 21/16 SVC = N/A	N/A	N/A	SV = N/A MPA = N/A SVC = 25	1.61	0.99	SV = 62/4 MPA = 31/25 SVC = 7.9	1.09	1.31	SV = 56/3 MPA = 38/23 SVC = 25.4
2	3.4	1.4	SV = 81/1 MPA = 15/9 SVC = N/A	N/A	N/A	SV = N/A MPA = N/A SVC < 12	2.46	0.98	SV = 86/2 MPA = 15/5 SVC = 6.2	2.05	1.26	SV = 73/2 MPA = 22/6 SVC = 6.8
3	2.5	0.53	AO = 92/47 MPA = 12 SVC = 9	N/A	N/A	AO = 70/36 MPA = 13 SVC = 17/13	2.14	0.55	AO = 90/44 MPA = 14/7 SVC = 8.4	1.82	1.04	AO = 79/40 MPA = 13/9 SVC = 13
4	0.99	1.45	LB = 89/48 MPA = N/A SVC = 5 IVC = N/A	N/A	1.55	LB = N/A MPA = 17/10 SVC = 18 IVC = 5	0.91	1.28	LB = 81/51 MPA = 24/12 SVC = 6.5 IVC = 6.3	0.59	1.8	LB = 55/42 MPA = 18/14 SVC = 15.6 IVC = 4.5

Note. AO, aorta; SV, single ventricle; MPA, main pulmonary artery; SVC, superior vena cava; IVC, inferior vena cava; LB, lower body; N/A, not available.

Study Limitations

The major drawback of this kind of analysis is the necessity to use many anatomic and hemodynamics parameters to characterize the hydraulic model of a specific patient. Their evaluation is a troublesome task, due to the impossibility of measuring those data during clinical investigations and procedures, except for the PAR and the SVR. Indeed, even in literature the great majority of data comes from *in vivo* measurements on animals [20, 21], while human data are scarce and usually refer to adults [12–15]. In order to simplify the model development, we adapted and scaled up an existing hydraulic parameter model of the fetal circulation, previously tested on pregnant women [10].

A further limitation of the discussed models may consist in the absence of any active regulation mechanisms, which generally operate when the equilibrium of a biological system is disturbed. Our models deal with severe pathologically altered situations and it appears reasonable to assume that such mechanisms have already failed, at least in part. However, one should note that the Frank–Starling mechanism that relates end-diastolic volume of the ventricle to stroke volume is implemented.

The model also does not take into account the respiratory rhythm effects on the SVC and IVC flow as well as the potential existence of stenoses at either right or left pulmonary artery bifurcations or at the main pulmonary bifurcation.

APPENDIX 1

Circulatory network. The generic district of the circulatory network of the lumped parameter model is composed of three elements (RCL block, Fig. 6). The flow is assumed to be one-dimensional and time-dependent and, according to the compliance definition, we can write for the ith block, the mass conservation law

$$Q_i(t) - Q_{i+1}(t) = \frac{dV_i(t)}{dt} = C_i \cdot \frac{dP_i(t)}{dt} \quad \text{(A1.1)}$$

and the momentum conservation law

$$P_{i-1}(t) - P_i(t) = L_i \cdot \frac{dQ_i(t)}{dt} + R_i \cdot Q_i(t), \quad \text{(A1.2)}$$

where $Q_i(t)$ and $Q_{i+1}(t)$ are the inlet and outlet volu-

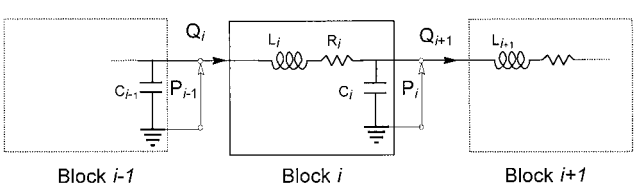

FIG. 6. The structure of the generic ith block of the hydraulic network, consisting of a resistance R_i, a compliance C_i, and an inertance L_i. P_i, pressure; Q_i, instantaneous volume flow rate.

metric blood flow rates, respectively, and $P_{i-1}(t) - P_i(t)$ the pressure drop across the block.

For the proximal pulmonary arterial districts (MPA, pRPA, and pLPA) Eq. (A1.2) becomes

$$P_{i-1}(t) - P_i(t) = L_i \cdot \frac{dQ_i(t)}{dt} + R_i \cdot Q_i(t) + K_{3D,i} \cdot Q^2(t) \quad (i = \text{MPA, pRPA, pLPA}), \quad \text{(A1.3)}$$

where the constant $K_{3D,i}$ takes into account the pressure losses in the anastomotic region [8].

Heart. The equations describing the ventricular behavior are

$$P_v(t) = U(t) + E(V_v,t) \cdot V_v(t) + R_v \cdot \frac{dV(t)}{dt} \quad \text{(A1.4)}$$

$$\frac{dV_v}{dt} = Q_{in}(t) - Q_{out}(t), \quad \text{(A1.5)}$$

where $P_v(t)$ and $V_v(t)$ indicate the instantaneous ventricular pressure and volume, respectively. Ventricular pressure depends also on the time derivative of the ventricular volume $dV_v(t)/dt$ [9]. $Q_{in}(t)$ and $Q_{out}(t)$ are the flows through the atrioventricular and arterial valves, respectively. These flows (synthetically indicated as $Q_{valv}(t)$) are related by a nonlinear relationship with the pressure drop $\Delta P_{valv}(t)$ across the valves,

$$\Delta P_{valv}(t) = K_{valv} \cdot Q_{valv}(t)^2, \quad \text{(A1.6)}$$

where K_{valv} is a constant parameter.

APPENDIX 2

We considered the systemic arterial oxygen availability or oxygen delivery (SAOA) a function of a group of hemodynamic and metabolic variables, namely, the pulmonary-to-systemic blood flow ratio (Q_p/Q_s), the systemic volume flow rate (Q_s), and the pulmonary venous oxygen saturation (Sat_{PV}).

With reference to Fig. 7, the basic equations that describe the oxygen transport from the lungs to the body are as follows:

$$Q_{SVC} \cdot C_{art}O_2 - \alpha_{UB} \cdot C\dot{V}O_2 = Q_{SVC} \cdot C_{SVC}O_2 \quad \text{(A2.1)}$$

$$Q_{IVC} \cdot C_{art}O_2 - \alpha_{LB} \cdot C\dot{V}O_2 = Q_{IVC} \cdot C_{IVC}O_2 \quad \text{(A2.2)}$$

$$Q_{MPA} \cdot C_{art}O_2 + Q_{SVC} \cdot C_{SVC}O_2 + S\dot{V}O_2 = Q_p \cdot C_{PV}O_2. \quad \text{(A2.3)}$$

Equations (A2.1) and (A2.2) state that the oxygen flow rates (ml oxygen/min) into the upper and lower body ($Q_{SVC} \cdot C_{art}O_2$ and $Q_{IVC} \cdot C_{art}O_2$) are decreased by the upper and lower body oxygen consumption ($\alpha_{UB} \cdot C\dot{V}O_2$ and $\alpha_{LB} \cdot C\dot{V}O_2$), leaving the reduced oxygen flow rate of the inferior vena cava ($Q_{IVC} \cdot C_{IVC}O_2$) returning to the left ventricle and the reduced oxygen flow rate of superior vena cava ($Q_{SVC} \cdot C_{SVC}O_2$) discharging into the pulmonary arteries through the caval anastomosis.

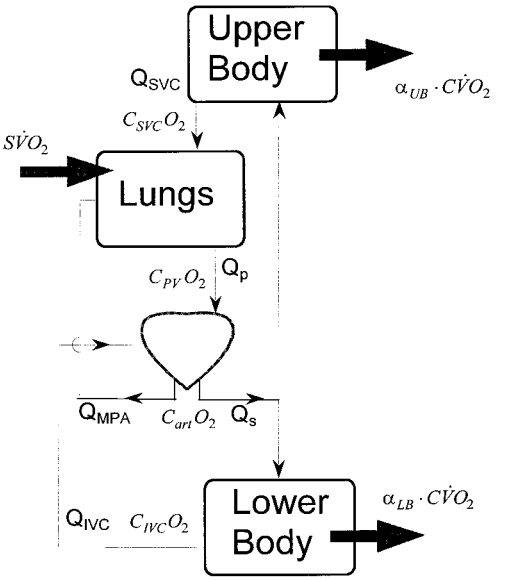

FIG. 7. Scheme for oxygen transport calculations.

Equation (A2.3) describes the oxygen flow balance into the lungs and states that the pulmonary venous oxygen flow rate ($Q_p \cdot C_{PV}O_2$) results from the sum of the oxygen flow rate into the pulmonary artery ($Q_{MPA} \cdot C_{art}O_2$) and that into the superior vena cava, plus the oxygen uptake in the lungs ($S\dot{V}O_2$).

Furthermore, it is

$$\alpha_{UB} + \alpha_{LB} = 1 \quad \text{(A2.4)}$$

$$Q_s = Q_{SVC} + Q_{IVC} \quad \text{(A2.5)}$$

$$Q_p = Q_{MPA} + Q_{SVC}. \quad \text{(A2.6)}$$

Last, according to mass conservation for steady-state condition, oxygen uptake in the lungs must be equal to oxygen consumption into the body, that is,

$$S\dot{V}O_2 = C\dot{V}O_2. \quad \text{(A2.7)}$$

By combining Eqs. (A2.1) to (A2.7), we obtain the systemic arterial oxygen availability (SAOA = $Q_s \cdot C_{art}O_2$) as a function of Q_s, Q_p/Q_s, $C_{PV}O_2$, and the metabolic oxygen consumption of lower body ($\alpha_{LB} \cdot C\dot{V}O_2$),

$$\mathrm{SAOA} = Q_s \cdot C_{PV}O_2 - \frac{(\alpha_{LB} \cdot C\dot{V}O_2)}{(Q_p/Q_s)} \quad \text{(A2.8)}$$

or

$$\mathrm{SAOA} = Q_s \cdot \frac{\mathrm{Sat}_{PV}}{100} \cdot \mathrm{OxCap} - \frac{(\alpha_{LB} \cdot C\dot{V}O_2)}{(Q_p/Q_s)}, \quad \text{(A2.9)}$$

where Sat_{PV} indicates the percentage of oxygen saturation of blood in the pulmonary veins and OxCap is the maximal oxygen capacity (ml oxygen/100 ml blood). Furthermore, the percentage of oxygen saturation of arterial blood Sat_{art} can be calculated

$$\mathrm{Sat}_{art} = \frac{\mathrm{SAOA}}{Q_s \cdot \mathrm{OxCap}} \cdot 100. \quad \text{(A2.10)}$$

APPENDIX 3: NOMENCLATURE

ABF	additional blood flow
AO	ascending aorta
ASD	atrial septal defect
BCPA	bidirectional cavopulmonary anastomosis
CFD	computational fluid dynamics
DIV	double inlet ventricle
IVC	inferior vena cava
LA	left atrium
LPA	left pulmonary artery
pLPA	proximal left pulmonary artery
MA	mitral atresia
MPA	main pulmonary artery
RA	right atrium
RPA	right pulmonary artery
pRPA	proximal right pulmonary artery
RVOTO	right ventricle outflow tract obstruction
SV	single ventricle
SVC	superior vena cava
TA	tricuspid atresia
BSA	body surface area (m^2)
CO	cardiac output (L/min)
HR	heart rate (bpm)
PAR	pulmonary arteriolar resistance (mm Hg · min/L)
SVR	systemic vascular resistance (mm Hg · min/L)
C_i	compliance of the ith block (ml/mm Hg)
$C\dot{V}O_2$	systemic oxygen consumption (ml O_2/min)
$E(V, t)$	time-varying, elastic term (mm Hg/ml)
$K_{valv,i}$	hydraulic dissipative coefficient for heart valves (mm Hg · s^2/ml^2)
$K_{3D,i}$	hydraulic dissipative coefficient due to local hemodynamics (mm Hg · s^2/ml^2)
L_i	inertance of the ith block (mm Hg · s^2/ml)
OxCap	maximal oxygen capacity (ml oxygen/100 ml)
$P(t)$	instantaneous pressure (mm Hg)
$P_v(t)$	instantaneous ventricular pressure (mm Hg)
$Q(t)$	instantaneous volume flow rate (ml/s)
$\dot{Q}(t)$	time derivative of the volume flow rate (ml/s^2)
Q_p/Q_s	pulmonary-to-systemic mean volume flow ratio
Q_r/Q_l	right-to-left lung mean volume flow ratio
Q_{SVC}/Q_p	superior vena caval-to-pulmonary mean volume flow ratio
R_i	resistance of the ith block (mm Hg · s/ml)
R_v	myocardium viscous term (mm Hg · s/ml)
SAOA	systemic arterial oxygen availability (ml oxygen/min)
Sat_{art}	percentage of arterial blood saturation (%)
Sat_{PV}	percentage of pulmonary vein blood saturation (%)
$S\dot{V}O_2$	oxygen uptake in the lungs (ml O_2/min)
t	time (s)
$U(t)$	isovolumic pressure generator (mm Hg)
$V(t)$	instantaneous compartmental volume (ml)
α	coefficient
μ	blood viscosity (g/(cm · s))
ρ	blood density (g/cm^3)
ΔP	pressure drop (mm Hg)

1 ml = 1 cm^3
1 L/min = 16.67 cm^3/s
1 mm Hg = 1333.2 g/(cm · s^2)

REFERENCES

1. Fontan, F., and Baudet, E. Surgical repair of tricuspid atresia. *Thorax* **26:** 240, 1971.
2. de Leval, M. R., Kilner, P., Gewillig, M., and Bull, C. Total cavopulmonary connection: A logical alternative to atriopulmonary connection for complex Fontan operations. *J. Thorac. Cardiovasc. Surg.* **96:** 682, 1988.
3. Haller, J. A., Adkins, J. C., Worthington, M., and Ravenhorst, J. Experimental studies on permanent bypass of the right heart. *Surgery* **59:** 1128, 1966.
4. de Leval, M. R., Dubini, G., Migliavacca, F., Jalali, H., Camporini, G., Redington, A., and Pietrabissa, R. Use of computational fluid dynamics in the design of surgical procedures: Application to the study of competitive flows in cavopulmonary connections. *J. Thorac. Cardiovasc. Surg.* **111:** 502, 1996.
5. Cape, E. G. Mathematical modeling in the evaluation and design of surgical procedures. *J. Thorac. Cardiovasc. Surg.* **111:** 499, 1996.
6. Migliavacca, F., de Leval, M. R., Dubini, G., and Pietrabissa, R. A computational pulsatile model of the bidirectional cavo pulmonary anastomosis: The influence of pulmonary forward flow. *J. Biomech. Eng.* **118:** 520, 1996.
7. Migliavacca, F., Dubini, G., Pietrabissa, R., and de Leval, M. R. Computational transient simulations with varying degree and shape of pulmonic stenosis in models of the bidirectional cavo pulmonary anastomosis. *Med. Eng. Phys.* **19:** 394, 1997.
8. Pennati, G., Migliavacca, F., Dubini, G., Pietrabissa, R., and de Leval, M. R. A mathematical model of circulation in the presence

of the bidirectional cavopulmonary anastomosis in children with a univentricular heart. *Med. Eng. Phys.* **19:** 223, 1997.

9. Avanzolini, G., Barbini, P., Cappello, A., and Cevese, A. Time-varying mechanical properties of the left ventricle: A computer simulation. *IEEE Trans. Biomed. Eng.* **32:** 756, 1985.
10. Pennati, G., Bellotti, M., and Fumero, R. Mathematical modelling of the human fetal cardiovascular system based on Doppler ultrasound data. *Med. Eng. Phys.* **19:** 327, 1997.
11. Rowlatt, U. F., Rimoldi, H. J. A., and Lev, M. The quantitative anatomy of the normal child's heart. *Pediatric Clin. North. Am.* **10:** 499, 1963.
12. Noordergraaf, A. Development of an analog computer for the human systemic circulatory system. In A. Noordergraaf (Ed.), *Circulatory Analog Computers.* Amsterdam: North-Holland, 1963. Pp. 29–44.
13. Westerhof, N., Bosman, F., De Vries, C. J., and Noordergraaf, A. Analog studies of the human systemic arterial tree. *J. Biomechanics* **2:** 121, 1969.
14. O'Rourke, M. F., and Avolio, P. Pulsatile flow and pressure in human systemic arteries: Studies in man and in multibranched model of the human systemic arterial tree. *Circ. Res.* **46:** 363, 1980.
15. Li, C. W., and Cheng, H. D. A nonlinear fluid model for pulmonary blood circulation. *J. Biomechanics* **26:** 653, 1993.
16. Santamore, W. P., Barnea, O., Riordan, C. J., Ross, M. P., and Austin, E. H. Theoretical optimization of pulmonary-to-systemic flow ratio after a bidirectional cavopulmonary anastomosis. *Am. J. Physiol.* **274:** H694, 1998.
17. Salzer-Muhar, U., Marx, M., Ties, M., Proll, E., and Wimmer, M. Doppler flow profiles in the right and left pulmonary artery in children with congenital heart disease and a bidirectional cavopulmonary shunt. *Pediatr. Cardiol.* **15:** 302, 1994.
18. Kobayashi, J., Matsuda, H., Nakano, S., Shimazaki, Y., Ikawa, S., Mitsuno, M., Takahashi, Y., Kawashima, Y., Arisawa, J., and Matsushita, T. Hemodynamic effects of bidirectional cavopulmonary shunt with pulsatile pulmonary flow. *Circulation* **84**(Suppl III): III-219, 1991.
19. Alvarado, O., Narayanswami, S., McKay, R., and Boyd, I. M. Cavopulmonary connection in region of atrioventricular septal defect with small right ventricle. *Ann. Thorac. Surg.* **55:** 729, 1993.
20. Rudolph, A. M., and Heymann, M. A. Fetal and neonatal circulation and respiration. *Annu. Rev. Physiol.* **36:** 187, 1974.
21. Rudolph, A. M., and Heymann, M. A. Cardiac output in the fetal lamb: The effects of spontaneous and induced changes of heart rate on right and left ventricular output. *Am. J. Obstet. Gynecol.* **124:** 183, 1976.